

SLS Symposium on Detectors and multiferroic materials

Tuesday, November 8, 2016

10:00 to 12:15, WBGB/019

10:00 Magnetolectric dynamic response of artificial multiferroic heterostructures

Jaianth Vijayakumar, L. Howald, N.S. Bingham, S.R.V. Avula, D. Bracher, S. Tatiana, O. Sendetskyi, M. Horisberger, L.J. Heyderman, Frithjof Nolting, C.A.F Vaz

10:30 Catalysis at a distance: single particle spectromicroscopy on nanofabricated model systems to visualize hydrogen spillover

Waiz Karim, Spreafico C., Kleibert A., Gobrecht J., VandeVondele J., Ekinici Y., van Bokhoven J.A.

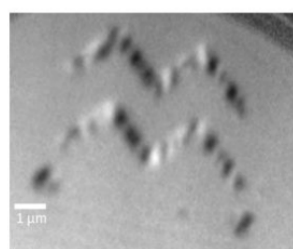
11:00 Coffee

11:15 Hybrid Pixel Detectors and Features of the PSI EIGER

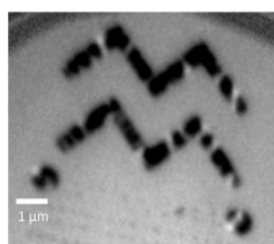
Erik Fröjdh on behalf of the SLS Detector Group.

11:45 Gotthard-II: A Silicon Micro-Strip Detector for the European XFEL

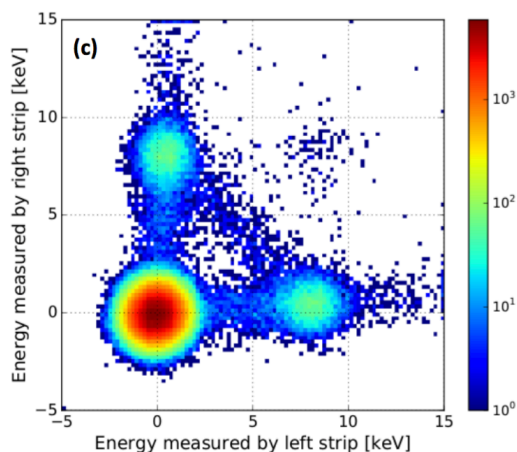
Jianguo Zhang, A. Bergamaschi, M. Brueckner, S. F. Cartier, R. Dinapoli, E. L. Froejdh, D. Greiffenberg, M. Kuster, D. Mayilyan, D. Mezza, A. Mozzanica, S. Redford, M. Ramilli, C. Ruder, X. Shi, D. Thattil, G. M. Tinti, M. Turcato and B. Schmitt



0V



+20V



Magnetolectric dynamic response of artificial multiferroic heterostructures

Jaianth Vijayakumar¹, L. Howald¹, N.S. Bingham^{2,3}, S.R.V. Avula¹, D. Bracher¹, S. Tatiana¹, O. Sendetskyi^{2,3}, M. Horisberger⁴, L.J. Heyderman^{2,3}, Frithjof Nolting¹, C.A.F Vaz¹

¹Swiss light source, Paul Scherrer Institute, Villigen 5232, Switzerland, jaianth.vijayakumar@psi.ch

²Laboratory for Mesoscopic Systems, Department of Materials, ETH Zurich, 8093 Zurich, Switzerland

³Laboratory for Micro- and Nanotechnology, Paul Scherrer Institute, 5232 Villigen PSI, Switzerland

⁴Laboratory of Neutron scattering and computing group, Paul Scherrer Institute, 5232 Villigen PSI, Switzerland

Artificial multiferroics consist of ferroelectric and ferromagnetic heterostructure, designed to exhibit a magnetolectric coupling between the two order parameters. By applying an electric field on the ferroelectric material the magnetisation of the ferromagnetic material can be controlled [1]. Our work aims at investigating the dynamic response of the magnetolectric coupling and fast electric field control of magnetism [2][3]. Here we present the results from the static measurements in strain-mediated coupling in BaTiO₃/Co and BaTiO₃/Ni multiferroic heterostructures. We demonstrate a change in magnetic anisotropy due to applied electric field in these systems. The electric field induces a strain through the piezo- or electrostrictive properties of the BaTiO₃, modifying the magnetic anisotropy in Co/Ni elements which are imaged using Photoemission electron microscopy (PEEM) shown in figure 1a. These results constitute a first step towards dynamic measurements. We also present the results obtained from electric field control of perpendicular magnetic anisotropy (PMA) in Si₃N₄/Pt/Co/Pt heterostructures. The result from the Magneto optic Kerr Effect measurements are shown in figure 1b showing a strong modulation of the PMA. PEEM results on similar structures showing modification of perpendicularly magnetised domain structures with applied electric field will also be presented, demonstrating the electric field control of magnetism in technologically relevant materials.

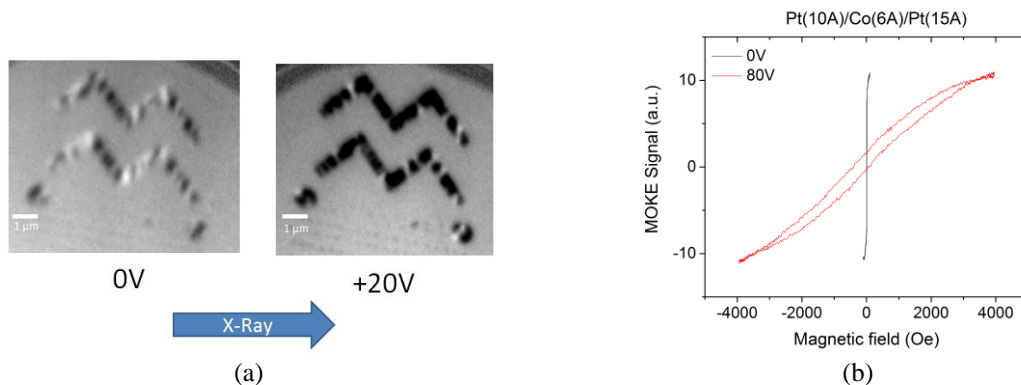


Figure 1: (a) PEEM images of BaTiO₃/Ni heterostructures before and after applying electric field showing clear changes in the magnetic contrast in the zig-zag structure (b) Magneto-optic Kerr effect measurement on Si₃N₄/Pt/Co/Pt heterostructures indicating a change in magnetic anisotropy with applied electric field

References

- [1] C. A. F Vaz, *Journal of Physics: Condensed Matter*, **24**, 333201(29pp) (2012)
- [2] C. A. F. Vaz and U. Staub, *Journal of Material Chemistry C*, **1**, 6731 (2013)
- [3] G.Srinivasan, *Annu. Rev. Mater. Res.*, **40**:153-78 (2010)

Catalysis at a distance: single particle spectromicroscopy on nanofabricated model systems to visualize hydrogen spillover

Waiz Karim^{1,2}, Clelia Spreafico², Armin Kleibert¹, Jens Gobrecht¹, Joost VandeVondele², Yasin Ekinci¹, Jeroen A. van Bokhoven^{1,2}

¹ Paul Scherrer Institute, Villigen PSI, Switzerland

² ETH Zurich, Zurich, Switzerland

Email : waiz.karim@psi.ch

We employ enhanced precision of top-down nanofabrication [1, 2] and single-particle *in-situ* X-ray absorption spectromicroscopy [2] to visualize hydrogen spillover, which is a critical phenomenon in heterogeneous catalysis [3]. Depending on the nature of the support, hydrogen spillover may occur in hydrogen catalysed reactions, which involve dissociative chemisorption of hydrogen onto a catalytic metal particle followed by migration of hydrogen atoms over the support. This eventually leads to the reaction of the hydrogen atoms with a species away from the hydrogen-splitting catalyst (Fig. 1a). Evidence of the occurrence of hydrogen spillover on non-reducible supports such as alumina is disputed, but has often been assumed to explain catalytic phenomena, while its occurrence on a reducible support like titania is generally accepted. Direct experimental proof of its existence does not exist due to the lack of well-defined model systems and the inability to observe the effect directly.

We develop novel model surfaces using extreme ultraviolet (EUV) lithography [1] and electron beam lithography (EBL) [2, 4] to achieve nanometer precision over particle size and its positioning. X-ray photoemission electron microscope (X-PEEM) at the Swiss Light Source (SLS) enables *in-situ* spectromicroscopy on individual iron particles prepared with nanofabrication [2, 4]. Fifteen pairs of nano-sized iron oxide and platinum particles at varying distances from each other starting at 0 nm to 45 nm are positioned on the same support with an accuracy of one nanometer, previously not achievable. The SEM image in Fig. 1b shows one of the pairs with a 25 nm distance. All pairs along with an iron oxide particle without any platinum in its proximity are probed simultaneously to visualize chemical reduction by hydrogen spillover. The spectra showed that hydrogen spillover on non-reducible alumina support depends on the distance from the catalyst and is relevant only at distances below 15 nm (Fig. 1c), occurring only on special sites. Maximum reduction occurs in the iron oxide particle overlapping with platinum, indicated by the highest intensity in the Fe L_{2,3} edge spectrum (P1 in Fig. 1c). As the distance from platinum increases, less reduction takes place and the pairs at higher distances, along with the iron oxide particle without platinum in its vicinity, have coinciding spectra which implies no spillover. Spillover on reducible titania support, which occurs via coupled electron-proton transfer, is uniform all over the support irrespective of distance. For the first time, distance dependence of hydrogen spillover has been experimentally visualized, and the hydrogen diffusion and migration mechanisms are elucidated by DFT calculations.

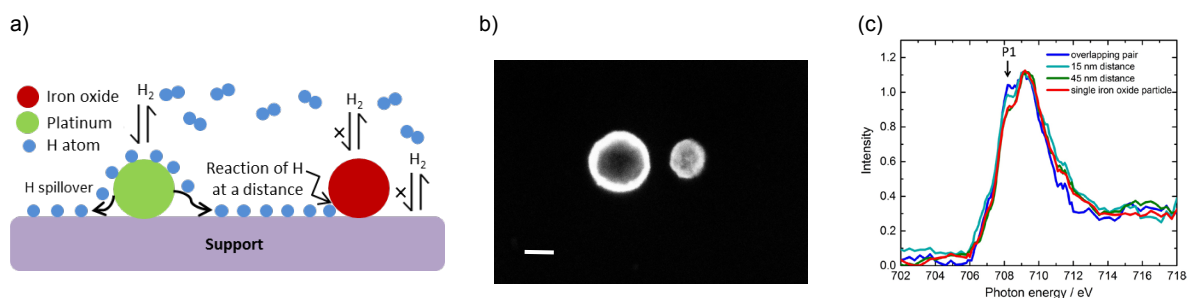


Figure 1. (a) Scheme of hydrogen spillover from platinum to an iron oxide particle over a titania or alumina support. (b) SEM image of a pair of iron oxide nanoparticle (60 nm diameter) and platinum nanoparticle (30 nm dimer) which are separated by 25 nm (scale bar: 40 nm). 15 such pairs at distances of 0 nm to 45 nm are fabricated on the same support. (c) Fe L₃ XAS spectra demonstrating the distance dependent reduction of the iron oxide particles on the alumina support for three selected pairs (an overlapping iron oxide and platinum pair, a pair with distances of 15 nm and 45 nm) and the iron oxide particle without platinum.

References

- [1] W. Karim, S. A. Tschupp, M. Oezaslan, T. J. Schmidt, J. Gobrecht, J. A. van Bokhoven, and Y. Ekinci, High-resolution and large-area nanoparticle arrays using EUV interference lithography, *Nanoscale* **7**, 7386 (2015).
- [2] W. Karim, A. Kleibert, U. Hartfelder, A. Balan, J. Gobrecht, J. A. van Bokhoven, and Y. Ekinci, Size-dependent redox behavior of iron observed by *in-situ* single nanoparticle spectro-microscopy on well-defined model systems, *Scientific Reports* **6**, 18818 (2016).
- [3] R. Prins, Hydrogen Spillover. Facts and Fiction, *Chemical Reviews* **112**, 2714 (2012).
- [4] W. Karim, S. Clelia, A. Kleibert, J. Gobrecht, J. VandeVondele, Y. Ekinci, and J. A. van Bokhoven, Support effects on hydrogen spillover, *Manuscript under review* (2016).

Hybrid Pixel Detectors and Features of the PSI EIGER

Erik Fröjdh on behalf of the SLS Detector Group.

The performance of hybrid pixel detectors depends on the radiation interaction and charge transport in the sensor layer, as well as on the readout ASIC. The first part of this talk will introduce hybrid pixel detectors and give an overview of the different steps in the signal generation process while the second part of the talk will focus on the new features of the PSI EIGER[1] detector.

Comparing with the PILATUS detector the most noticeable improvements with EIGER is a higher frame rate, of up to 23kHz, smaller pixels, $75 \times 75 \mu\text{m}^2$ and in FPGA count rate correction. The PSI EIGER system is also fully scalable giving the same performance regardless of the detector size, meaning that also the very high frame rates are available for example in the 9M detector built for cSAXS.

Threshold dispersion and energy resolution is also improved and after trimming a pixel to pixel threshold dispersion of less than 10e^- RMS have been achieved. The standard calibration [2] of EIGER using X-ray fluorescence in a lab setup is outlined and the different gain modes discussed. Figure 1 shows the count rate performance for an EIGER 500k module using 12.8 keV photons. The performance is similar to the PILATUS detector looking at per pixel values but with the smaller pixels EIGER is capable of operating in higher fluxes.

Finally a status update on current and future PSI EIGER detectors is given.

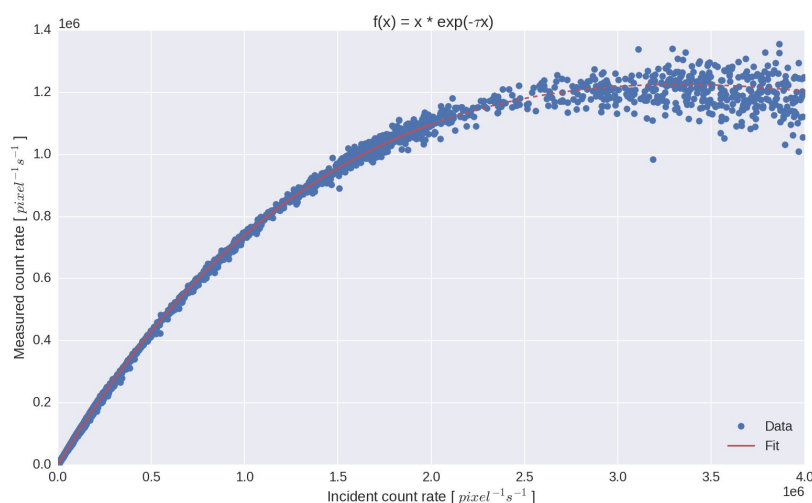


Figure 1: Measured vs. incoming count rate for 12.8 keV photons. Eiger 500k.

[1] R. Dinapoli et. al. *EIGER: Next generation single photon counting detector for X-ray applications*. NIMA Volume 650, Issue 1, 11 September 2011, Pages 79–83

[2] G. Tinti et. al. Performance of the EIGER single photon counting detector, JINST 10 March 2015

Gotthard-II: A Silicon Micro-Strip Detector for the European XFEL

J. Zhang^{1*}, A. Bergamaschi¹, M. Brueckner¹, S. F. Cartier¹, R. Dinapoli¹, E. L. Frojdh¹, D. Greiffenberg¹, M. Kuster², D. Mayilyan¹, D. Mezza¹, A. Mozzanica¹, S. Redford¹, M. Ramilli¹, C. Ruder¹, X. Shi¹, D. Thattil¹, G. M. Tinti¹, M. Turcato² and B. Schmitt¹

¹ Paul Scherrer Institut (PSI), 5232 Villigen PSI, Switzerland

² European X-ray Free Electron Laser Facility GmbH, 22761 Hamburg, Germany

The European X-ray Free-Electron Laser (XFEL.EU) [1], is currently being constructed in the Hamburg region and will be available for user operation in 2017. It will deliver extrashort, high intense X-ray pulses with a separation of 220 ns. The unique X-ray beam poses the following challenges to detectors used at the XFEL.EU: A dynamic range of 0, 1, ... 10^4 12.4 keV photons, a frame rate of 4.5 MHz, and last but not least radiation damage up to 1 GGy for 3 years of operation [2].

Gotthard-II is a 1-D micro-strip detector specifically developed for the XFEL.EU. It will be used not only as a spectrometer meeting all requirements mentioned above but also as a beam diagnostic tool with additional logic to generate veto signal for the other 2-D detectors in imaging experiments, like AGIPD and LPD. Gotthard-II makes use of silicon micro-strip sensor with a pitch of either 50 μm or 25 μm and with 1280 channels in total wire-bonded to ASIC chips with build-in ADCs and memories for a continuous readout of frames and hit information generated by each X-ray pulse.

The performance of existing prototypes has been investigated extensively. In this work, the results regarding to noise, dynamic range and strip-to-strip coupling by means of infrared laser and X-rays will be shown and its influence on the design of Gotthard-II discussed. The architecture of the final ASIC will be presented.

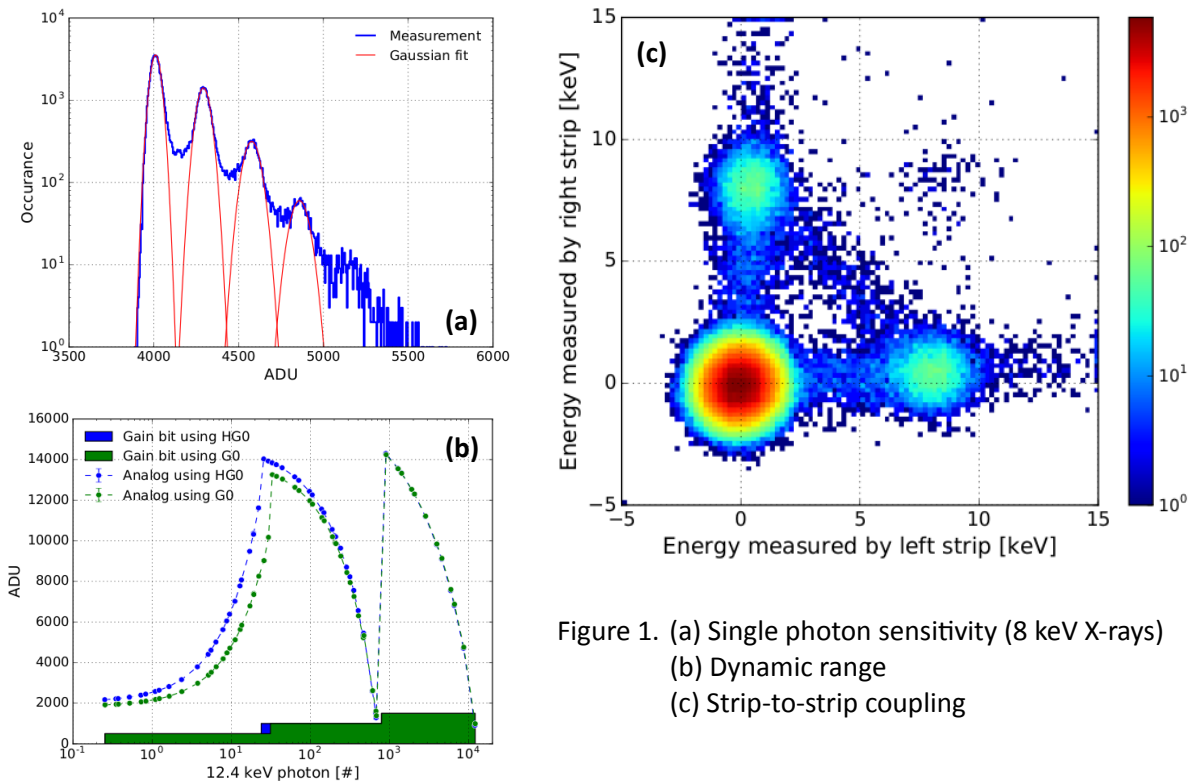


Figure 1. (a) Single photon sensitivity (8 keV X-rays)
(b) Dynamic range
(c) Strip-to-strip coupling

[1] Webpage of XFEL.EU: <http://www.xfel.eu>.

[2] Graafsma, H. (2009). J. Instrum. 4, P12011.

* jiaguo.zhang@psi.ch